View Article Online
View Journal

Journal of
Materials Chemistry C
Materials for optical, magnetic and electronic devices

This article can be cited before page numbers have been issued, to do this please use: J. Hua, M. Xu, K. Kong, H. Ding, Y. Chu, S. Zhang, F. Yu, H. Ye and Y. Hu, *J. Mater. Chem. C*, 2020, DOI: 10.1039/C9TC04175C.

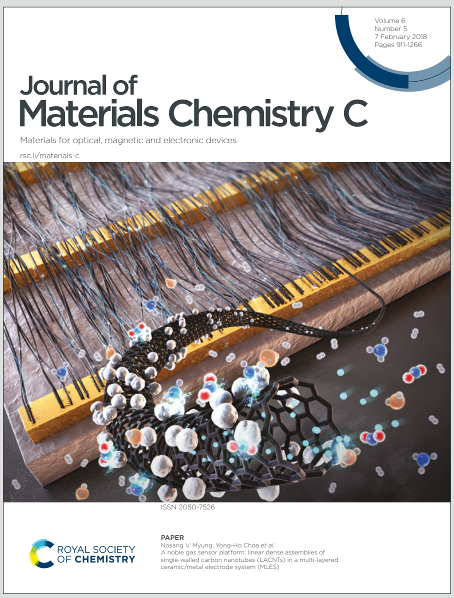

ROYAL SOCIETY OF CHEMISTRY

rsc.li/materials-c

View Article Online
DOI: 10.1039/C9TC04175C

COMMUNICATION

Quinacridone-pyridine dicarboxylic acid based donor-acceptor supramolecular nanobelts for significantly enhanced photocatalytic hydrogen production

Received 00th January 20xx,
Accepted 00th January 20xx

DOI: 10.1039/x0xx00000x

Mengyu Xu[a], Kangyi Kong[a], Haoran Ding[a], Yanmeng Chu[b], Shicong Zhang[a], Fengtao Yu[a], Haonan Ye[a], Yue Hu[b] and Jianli Hua*[a]

The self-assembled nanobelt photocatalysts (SQAP-C4 and SQAP-C8) with quinacridone containing butyl and octyl side chains as electron donor and pyridine dicarboxylic acid as acceptor were firstly developed for efficient hydrogen evolution. SQAP-C4 without the loading of cocatalyst Pt exhibited superior H_2 evolution reaction of 656 μmol $h^{-1}g^{-1}$ and excellent stability.

With the advent of the energy crisis, hydrogen has become a potential energy source that can alleviate the energy crisis. Interestingly, the natural light synthesis system can convert sunlight into hydrogen energy by integrating the π-π conjugate chromophore and active catalytic center.[1, 2] Therefore, organic synthetic materials containing π-π chromophores may have certain advantages in artificial photosynthetic systems.[3] Small organic molecules containing π-π chromophores have been used in organic optoelectronic materials as well as in solid state semiconductors.[4-5] While the self-assembled systems with large electron delocalization are reported, which are applied in charge transport materials and water splitting.[6,7]

Quinacridone (**QA**) and its derivatives, as well-known red-violet dyes with large π-π chromophore, have many excellent advantages such as chemical stability, good carrier mobility, thermal stability and wide ultraviolet-visible absorption range.[8,9] Therefore, it is widely used in various optoelectronic devices, including organic solar cells,[10] light-emitting diodes,[11-13] and field effect transistors.[14-16] It is important to note that in most studies, quinacridone derivatives are primarily used as charge transport materials[10] or photosensitizers.[17] Neverthless, the problems of fast charge recombination and hydrophobic resulting from strong rigidity limit the application of **QA** system in the photocatalytic water splitting. Interestingly, pyridine-2,6-dicarboxylic acid (**PDA**) with two carboxylic acid groups exhibits pretty hydrophilic.[18] What's more, the pyridine ring with an electron-deficient structure (an electron acceptor) can form a built-in diploe combined with **QA** (an electron donor) by donor-acceptor (D-A) interaction.[14, 19,20] Due to D-A effect, the charge separation efficiency is improved.[20-22] Based on above analysis, two D-A **QA**-based supramolecular catalysts (**SQAP-C4** and **SQAP-C8**) with different length of butyl and octyl chains have been successfully synthesized and used for hydrogen evolution. Furthermore, the different length of alkyl chains may affect the supramolecular packing which further has an influence on photocatalytic activity.

It is the first time that the self-assembled quinacridone derivative is used for hydrogen evolution. Surprisingly, the two supramolecular photocatalysts can achieve a gratifying hydrogen evolution reaction (HER) without loading the cocatalyst Pt, in which **SQAP-C4** exhibits HER of ca. 656 μmol h^{-1} g^{-1}. In addition, the photocatalytic activity of **SQAP-C4** with Pt cocatalyst loaded was also observed, which is about 3 times (1.93 mmol h^{-1} g^{-1}) higher than **SQAP-C4** without Pt. Moreover, the supramolecular photocatalysts show excellent stability and the photocatalytic performance is not decayed after 15 hours of illumination. Hence, two new **QA**-**PDA** self-assembled nanobelt photocatalysts provide a new idea for the design of organic photocatalysts.

The synthetic route of two **QA**-**PDA** with butyl and octyl chain(termed as **QAP-C4** and **QAP-C8**) is shown in Scheme S1. And the self-assembled S**QAP-C4** and S**QAP-C8** nanobelts were synthesized through a facile and economic acid-base neutralization reaction method by using triethanolamine (TEOA) as base and HCl as acid. The process is schematically illustrated in Scheme 1.

The scanning electron microscopy (SEM) and transmission electron microscopy (TEM) can be used to determine how alkyl chain variations altered supramolucles morphologies and molecular packing. As shown in SEM images (Fig. 2a~2b), the self-assembled supramolecules of **SQAP-C4** and **SQAP-C8** were

[a] *Key Laboratory for Advanced Materials, Institute of Fine Chemicals, School of Chemistry and Molecular Engineering, East China University of Science and Technology, 130 Meilong Road, Shanghai, 200237, PR China.*
Email: jlhua@ecust.edu.cn
[b] *Michael Grätzel Center for Mesoscopic Solar Cells, Wuhan National Laboratory for Optoelectronics, Huazhong University of Science and Technology, Wuhan 430074, Hubei, PR China.*
Electronic Supplementary Information (ESI) available: [details of any supplementary information available should be included here]. See DOI: 10.1039/x0xx00000x

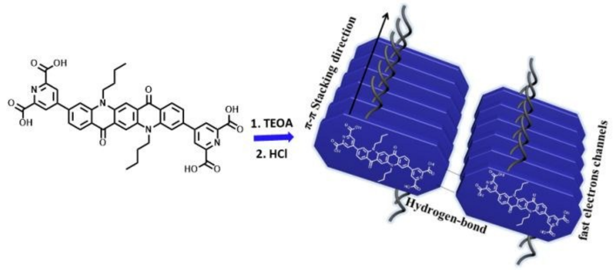

Scheme 1. Schematic illustration of formation of the self-assembled **SQAP-C4** nanostructures

nanoribbon formed by π-π stacking and hydrogen bond, in which **SQAP-C4** showed shorter nanoribbon compared with **SQAP-C8**. TEM images revealed that **SQAP-C4** assembled into a thin and narrow nanobelt like willow leaves with a width of about 50 nm and a length of hundreds of nanometers (Fig. 2c ~2d). In contrast, **SQAP-C8** formed exclusively wide and long nanobelts, which was hundreds of nanometers to micrometers in length and about 100 nm in width. The one possible explanation may be that the steric hindrance of the octyl chains prevented closer π-π stacking and probably contributed to the formation of *J*-aggregation.[23]

It is well known that thin layer structure is a favorable parameter for photocatalytic performance because it can provide more react sites and shorter diffusion distance.[24, 25] What's more, the shorter distance to the surface facilitates the migration of photogenerated carriers.[3] From the AFM image (Fig. S1 and Fig. S2), we can observe that the self-assembled **SQAP-C4** crystalized well with a thinner thickness of 37 nm, while the layer thickness of supramolecule **SQAP-C8** was 55 nm. Hereby, the supramolecule morphologies clearly changed by only varying the alkyl chain length of **QA** moiety and **SQAP-C4** showed a thinner and narrow nanobelt structure which may be beneficial to photocatalysis.

The X-ray diffraction (XRD) measurement was used to further evaluate the π-π interaction within the supramolecules. A slightly wide peak around 25° in **QAP-C4** and **QAP-C8** can be seen, indicating a certain degree of π-π interaction in the precursors (Fig.S7-S8). As for supramolecules, it can be seen that **SQAP-C4** showed a peak at 2θ = 25.40°which corresponds to the layer-to-layer spacing (*d*-spacing of π-π stacking) of 3.5 Å.[14] In addition, the peaks of 2θ = 31.64° and 2θ = 45.42° with *d*-spacing of 2.82 Å and 1.99 Å indicated the possible formation of hydrogen-bond, respectively.[26] As for the self- assembled **SQAP-C8**, it only showed one peak at 2θ = 25.30°corresponded to 3.52 Å which could be assigned to further π-π stacking distance.[14] This may be due to the longer octyl chain will wrap around chromophore hindering the formation of hydrogen bond and leading to further π-π stacking distance.[3] And the result revealed that the **SQAP-C4** self-assemble tighter and has improved regularity from π-π stacking interaction and hydrogen bond formation resulting from the shorter length of butyl chain. The smaller *d*-spacing of π-π stacking in the **SQAP-C4** nanobelts also meant a higher electron cloud overlap density which is expected to benefit the migration of charge carriers.[3, 27, 28]

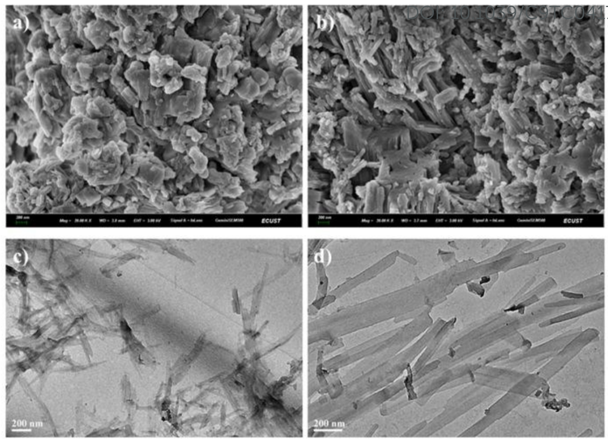

Fig. 2 SEM images of **SQAP-C4** (a) and **SQAP-C8** (b); TEM images of **SQAP-C4** (c) and **SQAP-C8** (d).

The Raman spectra were performed to further determine the π-π interaction between the supramolecules (Fig. 3b). According to previous research,[29] the peak of 1602 cm^{-1} corresponds to the in-plane C=C/C-C stretching/shrinking of the quinacridone aromatic ring core coupled to the C=O antisymmetric stretching, which was sensitive to the π-π stacking effect. However, the peak at 1359 cm^{-1} attributed to C-H in plane bending was not sensitive to intermolecular interactions. Thus, the ratio of 1602 cm^{-1}/1359 cm^{-1} Raman intensity can be used as an effective marker to evaluate the π-π interaction. The ratio of **SQAP-C4** (1.35) and **SQAP-C8** (1.34) was higher than the **QAP-C4** (1.17) and **QAP-C8** (1.17) respectively, which revealed the improvement of π-π interaction between the suparmolecules. Thus, there is better regularity in suparmolecules and it can form fast-transporting channels in the π–π stacking direction and the carriers can be transported by the channels.

Absorbance spectra of the monomers **QAP-C4** and **QAP-C8** were measured in DMSO (Fig. S3 and Fig. S4) and the optical properties of **QAP-C4, QAP-C8, SQAP-C4** and **SQAP-C8** were

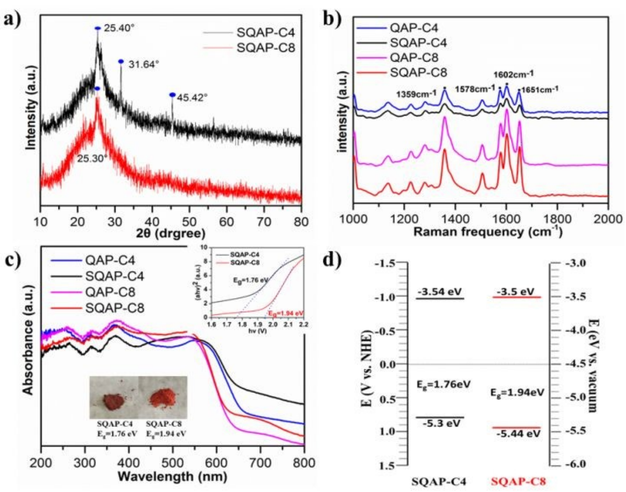

Fig. 3 (a) XRD patterns of **SQAP-C4** and **SQAP-C8** powder. (b) Raman spectra of **QAP-C4**, **QAP-C8**, **SQAP-C4** and **SQAP-C8** powder. (c) UV–vis diffuse reflection spectra of **QAP-C4, QAP-C8, SQAP-C4** and **SQAP-C8** (Inset: the corresponding colors and the Tauc plots.) (d) Band diagram for **SQAP-C4** and **SQAP-C8**.

DOI: 10.1039/C9TC04175C

measured by UV-vis diffuse reflection spectra (DRS) (Fig.3c). Firstly, owing to the π-π stacking, the electronic clouds overlapped and isolated molecule energy level was linear combined to the semiconductor energy band which presented an absorption edge of 650 nm, indicating their excellent ability of response to visible light.[30] Secondly, the absorption peaks of monomers **QAP-C4** and **QAP-C8** in DMSO are almost coincident. However, there is an obvious red-shifted in the DRS spectrum of **SQAP-C4** compared with **SQAP-C8,** which resulted from more closely π-π stacking of **SQAP-C4**.[31] What's more, the red-shifted of **SQAP-C4** revealed broader spectrum absorption region. Thirdly, with the contents of water increased, the monomer molecules began to aggregate, and the red shift of the absorption peak may indicate *J*-aggregation between supramolucles (Fig. S3 and Fig. S4).[3,32] Finally, compared with **3a** and **3b**, **PQA-C4** and **PQA-C8** have a new absorption peak between 350 and 450 nm, respectively. This result indicated the effect of intramolecular charge transfer between the **QA** skeleton and the **PDA** group, which further proved the D-A interaction.[10] What's more, as shown in Table S2, the theoretical calculation results showed **SQAP-C4** has a larger dipole moment of 0.67 Debye which proved a better ability of charge separation.

According to the Tauc plots (Fig.3c, inset), the band gap energy of the **SQAP-C4** and **SQAP-C8** was calculated to be 1.76 eV and 1.94 eV, respectively. According to the calculation result, the HOMO of **SQAP-C4** and **SQAP-C8** was measured to be -5.30 eV and -5.44 eV (vs vacuum), respectively. As a result, the LUMO of **SQAP-C4** and **SQAP-C8** should be -3.54 eV and –3.50 eV from E_{HOMO} + Eg (Fig. 3d). Because the LUMO of supramolecules was higher than that of H^+/H_2 (-4.5 eV), the supramolecules have enough reducing capacity to react with H^+ producing H_2 on the surface of photocatalyst.

To further confirm the structure of **SQAP-C4** and **SQAP-C8**, the Fourier transform infrared (FT-IR) was carried out (Fig. S5 and Fig. S6). The peak of **6a** and **6b** at 1743 cm^{-1} was attributed to the C=O stretching vibration of pyridine dicarboxylic ester group. And this peak disappeared in **QAP-C4** and **QAP-C8**, indicating that the ester groups were all hydrolyzed to carboxyl groups. And the peak of 1720 cm^{-1}, 1724 cm^{-1}, 1725 cm^{-1}, 1726 cm^{-1} were attributed to the C=O stretching vibration of quinacridone core. A series of peaks ranged from 1270 cm^{-1} to 1292 cm^{-1} were attributed to the C-N stretching vibration of the quinacridone core. And the peaks ranged from 1625 cm^{-1} to 1633 cm^{-1} were assigned to the characteristic stretching vibration of C=N of pyridine. Interestingly, it can be clearly seen from Table S1 that the vibration peaks of self-assembled **SQAP-C4** and **SQAP-C8** shifted to a higher wave numbers compared to the monomer of **QAP-C4** and **QAP-C8,** which further proved the increase of the π-π conjugated structure in supramolecules of **SQAP-C4** and **SQAP-C8**.[33]

Their photocatalytic H_2 production without cocatalysts was tested under visible light irradiation in L-ascorbic acid (AA) aqueous solution as sacrificial agents (Fig. 4a, Fig.S15). The H_2 production rate were 394, 35.6, 656, 177 μmol g^{-1} h^{-1} (λ > 400 nm) for **QAP-C4**, **QAP-C8**, **SQAP-C4** and **SQAP-C8,** respectively, in which **SQAP-C4** was 3.7 times higher than that of **SQAP-C8**.

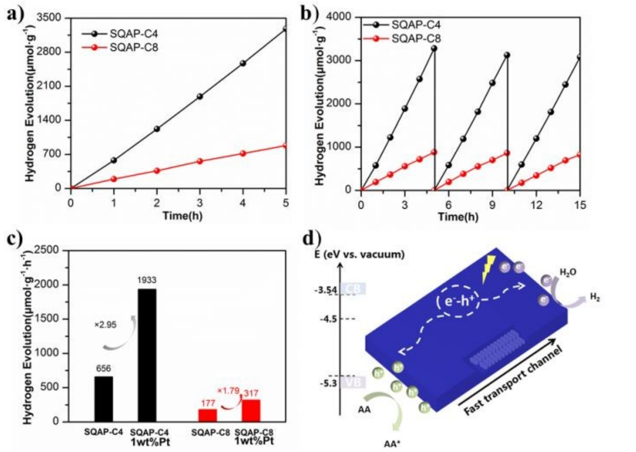

Fig. 4 (a)Time-dependent photocatalytic hydrogen evolution over **SQAP-C4** and **SQAP-C8**. (b) The reaction rate comparison of **SQAP-C4**, **SQAP-C8**, Pt-loaded **SQAP-C4** and Pt-loaded **SQAP-C8**. (c) Photostability for hydrogen evolution of the **SQAP-C4** and **SQAP-C8**. Reaction conditions: 50 mL water, 3 g AA, 30 mg photocatalyst under visible-light (400 nm < λ< 780 nm). (d) Proposed electron transfer mechanism of supramolecular **SQAP-C4** for photocatalytic H_2 production.

The excellent performance can be attributed to the fact **SQPA-C4** has wider spectrum and more efficient photoinduced charge separation resulting from the closer π-π stacking distance and larger dipole moment. In addition to the photocatalytic properties, the stability of **SQAP-C4** and **SQAP-C8** was also evaluated in three consecutive runs of accumulatively 15 h with intermittent evacuation every 5 h under visible light irradiation (Fig. 4b). There was no noticeable attenuation in H_2 production rate after 3 cycling tests, suggesting the high stability of **SQAP-C4** and **SQAP-C8**. The stabilities of catalysts were further verified by XRD, FT-IR and Raman data (Fig.S16-S18). In addition, we also measured the hydrogen production of **SQAP-C4** with 1wt% Pt. which reached 1933 μmol g^{-1} h^{-1}. From TEM image (Fig. S14), we can observe that Pt particle was distributed on the surface of **SQAP-C4** uniformly. And it was 2.95 times more than that of **SQAP-C4** without Pt. While the **SQAP-C8** with 1wt% Pt (317 μmol g^{-1} h^{-1}) was only 1.79 times than that of **SQAP-C8** without Pt (Fig. 4c). The performances were compared with the self-assembled materials recently reported (Table S3 in the Supporting Information). In most of the studies already reported, a cocatalyst is needed to reduce the overpotential, but the introduction of a cocatalyst results in a large consumption of precious metals. It should be noted that the HER of 656 μmol h^{-1} g^{-1} for **SQAP-C4** without the loading of cocatalyst Pt is comparable to or even higher than that of most reported self-assembled photocatalysts shown in Table S4. Thus, the **SQAP-C4** provides a resource-saving and environmental friendly photocatalyst.

In order to further explore the electron transfer kinetics of supramolecules, photoluminescence (PL) spectroscopy test was conducted. As shown in Fig. S11, **SQAP-C8** showed a strong emission peak at 649 nm, indicating the fast recombination of photogenerated carriers. In contrast, **SQAP-C4** exhibited lower fluorescence intensity with an emission peak at 652 nm. The lower fluorescence intensity revealed superior charge separation ability of **SQAP-C4.** The transient photocurrent responses (*I*–*t*) was further performed and confirmed that **SQAP-C4** had promoted photoresponsive ability and photo-generated carrier separation ability compared with **SQAP-C8**. Fig. S10 illustrated the results of electrochemical impedance spectroscopic (EIS) measurements. In general, smaller charge transfer resistance, the faster interfacial electron transfer. Thus **SQAP-C4** had better photocatalyst capability.

Based on above experimental results, a possible mechanism of hydrogen production by supramolecular is proposed. Take **SQAP-C4** as an example as shown in Fig. 4(d), photogenerated carriers can be generated under visible-light irradiation, and carriers are separated under the built-in electric field resulting from D-A interaction, and then transmitted through the fast channel formed by π-π stacking, after that electrons are transported to the surface of the photocatalyst, then captured by protons in the water and hydrogen produced.

Conclusions

In summary, a novel self-assembled photocatalyst based on quinacridone as electron donor and pyridine dicarboxylic acid as acceptor moiety was successfully constructed. To the best of our knowledge, this is the first time that the quinacridone derivative photocatalysts were developed for efficient and stable photocatalytic hydrogen evolution by self-assembly. The degree of self-assembled depends strongly on length of alkyl chain the lactam N positions of the quinacridone moiety, which leads to differences in the absorption spectrum and charge separation efficiency of supramolecules. The closer π-π stacking of **SQAP-C4** made it exhibit broader visible light absorption spectrum and improve charge separation capability, which resulting in the enhancement of photocatalyst performance with a hydrogen evolution rate of 656 μmol g^{-1} h^{-1} without any precious metal addition under visible light irradiation (λ > 400 nm). Moreover, **SQAP-C4** can achieve 1.93 mmol g^{-1} h^{-1} with 1 wt% Pt as cocatalyst. This self-assembly quinacridone photocatalysts offer a new strategy for optimizing the activity and stability of organic photocatalytic systems.

This work was supported by the National Natural Science Foundation of China (21971064, 21421004, and 21572062), the Fundamental Research Funds for the Central Universities (50321101918001 and 222201717003) and the Programme of Introducing Talents of Discipline to Universities (B16017). The authors thank Research Center of Analysis and Test of East China University of Science and Technology for the help on the characterization.

Conflicts of interest

There are no conflicts to declare.

Notes and references

1. A. Amunts, H. Toporik, A. Borovikova and N. Nelson, *J. Biol. Chem.*, 2010, **285**, 3478–3486.
2. C. E. Lubner, R. Grimme, D. A. Bryant and J. H. Golbeck, *Biochemistry*, 2010, **49**, 404–414.
3. A. S. Weingarten, R. V. Kazantsev, A. R. Koltonow and S. I. Stupp, *J. Am. Chem. Soc.*, 2015, **137**, 15241–15246.
4. M. Sofos, J. Goldberger, D. A. Stone, D. J. Herman, W. W. Tsai, L. J. Lauhon and S. I. Stupp, *Nat. Mater.*, 2009, **8**, 68–75.
5. S. Loser, C. J. Bruns, H. Miyauchi, A. Facchetti, S. I. Stupp and T. J. Marks, *J. Am. Chem. Soc.*, 2011, **133**, 8142–8145.
6. K. Okeyoshi and R. Yoshida, *Adv. Funct. Mater.*, 2010, **20**, 708–714.
7. K. Kong, S. Zhang, Y. Chu, Y. Hu, F. and J. Hua, *Chem. Comm.*, 2019, **55**, 8090–8093.
8. H.-J. Song, D.-H. Kim, E.-J. Lee, S.-W. Heo, J.-Y. Lee and D.-K. Moon, *Macromolecules*, 2012, **45**, 7815–7822.
9. C. Wang, Z. Zhang and Y. Wang, *J. Mater. Chem. C*, 2016, **4**, 9918–9936.
10. H. D. Pham, S. M. Jain, M. Li, S. Manzhos, H. Wang, J. R. Durrant and P. Sonar, *J. Mater. Chem. A*, 2019, **7**, 5315–5323.
11. J. Wang, Y. Zhao, C. Dou, H. Sun, P. Xu, K. Ye, J. Zhang, S. Jiang, F. Li and Y. Wang, *J. Phys. Chem. B*, 2007, **111**, 5082–5089.
12. P. G. Lacroix, T. Hayashi, T. Sugimoto, K. Nakatani and V. Rodriguez, *J. Phys. Chem. C*, 2010, **114**, 21762–21769.
13. K. D. Theriault, C. Radford, M. Parvez, B. Heyne and T. C. Sutherland, *Phys. Chem. Chem. Phys.*, 2015, **17**, 20903–20911.
14. M. Akita, I. Osaka and K. Takimiya, *Materials* 2013, **6**, 1061–1071.
15. C. Wang, S. Wang, W. Chen, Z. Zhang, H. Zhang and Y. Wang, *RSC Advances*, 2016, **6**, 19308–19313.
16. J. Jia, C. Hu, Y. Cui, Y. Li, W. Wang, L. Han, Y. Li and J. Gao, *Dyes and Pigments*, 2018, **149**, 843–850.
17. J. Jia, Y. Li, W. Wang, C. Luo, L. Han, Y. Li and J. Gao, *Dyes and Pigments*, 2017, **146**, 251–262.
18. H. Xiao, H. Li, M. Chen and L. Wang, *Dyes and Pigments*, 2009, **83**, 334–338.
19. J. Wang, W. Shi, D. Liu, Z. Zhang, Y. Zhu and D. Wang, *Appl. Catal. B-Environ.*, 2017, **202**, 289–297.
20. K. Nath, M. Chandra, D. Pradhan and K. Biradha, *ACS Appl. Mater. Interfaces*, 2018, **10**, 29417–29424.
21. Q. Ou, Y. Zhang, Z. Wang, J. A. Yuwono, N. V. Medhekar, H. Zhang and Q. Bao, *Adv. Mater.*, 2018, **30**, e1705792.
22. L. Li, Z. Cai, Q. Wu, W. Y. Lo, N. Zhang, L. X. Chen and L. Yu, *J. Am. Chem. Soc.*, 2016, **138**, 7681–7686.
23. T. Zhou, T. Jia, B. Kang, F. Li, M. Fahlman and Y. Wang, *Adv. Energy Mater.*, 2011, **1**, 431–439.
24. L. Wang, Y. Wan, Y. Ding, S. Wu, Y. Zhang, G. Zhang, Y. Xiong, X. Wu, J. Yang and H. Xu, *Adv. Mater.*, 2017, **29**, 1702428.
25. Y. Xiao, G. Tian, W. Li, Y. Xie, B. Jiang, C. Tian, D. Zhao and H. Fu, *J. Am. Chem. Soc.*, 2019, **141**, 2508–2515.
26. O. Guillermet, M. Mossoyan-Déneux, M. Giorgi, A. Glachant and J. C. Mossoyan, *Thin Solid Films*, 2006, **514**, 25-32.
27. P. Chen, L. Blaney, G. Cagnetta, J. Huang, B. Wang, Y. Wang, S. Deng and G. Yu, *Environ. Sci. Technol*, 2019, **53**, 1564–1575.
28. J. Yang, H. Miao, W. Li, H. Li and Y. Zhu, *J. Mater. Chem. A*, 2019, **7**, 6482–6490.
29. R. Singh, E. Giussani, M. M. Mróz and P. E. Keivanidis, *Organic Electronics*, 2014, **15**, 1347–1361.
30. Z. Zhang, Y. Zhu, X. Chen, H. Zhang and J. Wang, *Adv. Mater.*, 2019, **31**, e1806626.
31. X. Chen, Z. Zhang, Z. Ding, J. Liu and L. Wang, *Angew. Chem. Int. Ed.*, 2016, **55**, 10376–10380.
32. C. Dou, D. Li, H. Gao, C. Wang, H. Zhang and Y. Wang, *Langmuir*, 2010, **26**, 2113–2118.

33. H. F. Ji, R. Majithia, X. Yang, X. Xu and K. More, *J. Am. Chem. Soc.*, 2008, **130**, 10056–10057.

View Article Online
DOI: 10.1039/C9TC04175C

View Article Online
DOI: 10.1039/C9TC04175C

Graphical Abstract

Quinacridone-pyridine dicarboxylic acid based donor-acceptor supramolecular nanobelts for significantly enhanced photocatalytic hydrogen production

*Mengyu Xu, Kangyi Kong, Haoran Ding, Yanmeng Chu, Shicong Zhang, Fengtao Yu, Haonan Ye, Yue Hu and JianLi Hua**

In this paper, The self-assembled nanobelt photocatalysts (**SQAP-C4** and **SQAP-C8**) with quinacridone containing butyl and octyl side chains as electron donor and pyridine dicarboxylic acid as acceptor were firstly developed for efficient hydrogen evolution. **SQAP-C4** without the loading of cocatalyst Pt exhibited superior H_2 evolution reaction of 656 μmol $h^{-1}g^{-1}$ and excellent stability.